

Single additive mechanism predicts lateral interactions effects—computational model

HAVA MATICHIN,^{1,*} SHMUEL EINAV,² AND HEDVA SPITZER¹

¹School of Electrical Engineering, Tel-Aviv University, Tel Aviv, Israel

²Department of Biomedical Engineering, Tel-Aviv University, Tel Aviv, Israel

*Corresponding author: havi.mati@gmail.com

Received 18 September 2014; revised 16 September 2015; accepted 17 September 2015; posted 21 September 2015 (Doc. ID 221826); published 2 November 2015

The mechanism underlying the lateral interactions (LI) phenomenon is still an enigma. Over the years, several groups have tried to explain the phenomenon and suggested models to predict its psychophysical results. Most of these models comprise both inhibitory and facilitatory mechanisms for describing the LI phenomenon. Their studies' assumption that a significant inhibition mechanism exists is based on the classical interpretation of the threshold elevation perceived in psychophysical experiments. In this work, we suggest a different interpretation of the threshold elevation obtained experimentally. Our model proposes and demonstrates how a facilitatory additive mechanism can solely predict both the facilitation and "inhibition" aspects of the phenomenon, without the need for an additional inhibitory mechanism, at least for the two flankers' configurations. Though the model is simple it succeeds to predict the LI effect under a large variety of stimuli configurations and parameters. The model is in agreement with both classical and recent psychophysical and neurophysiological results. We suggest that the LI mechanism plays a role in creating an educated guess to form a continuation of gratings and textures based on the surrounding visual stimuli. © 2015 Optical Society of America

OCIS codes: (330.1800) Vision—contrast sensitivity; (330.1880) Detection; (330.4060) Vision modeling; (330.4270) Vision system neurophysiology; (330.7310) Vision.

<http://dx.doi.org/10.1364/JOSAA.32.002247>

1. INTRODUCTION

The visibility of an oriented stimulus, such as a Gabor pattern, may be modified by the presence of nearby collinear flankers (first introduced by Polat and Sagi in 1993 [1]). It was reported that these lateral interactions (LIs) can be manifested by both facilitation and inhibition [1]. More specifically, a stimulus that is subthreshold when presented alone may become noticeable when surrounded by similarly oriented flankers (i.e., lateral facilitation). On the other hand, the above-mentioned flankers at closer proximity can lead to the opposite phenomenon; superthreshold stimuli become unnoticeable (i.e., lateral inhibition).

It has been shown that the role of the distance between the flankers and the central target is crucial for the expression of threshold facilitation or inhibition and their magnitudes (Fig. 3 in [1]). Threshold decrement (facilitation) occurs in the case of collinear configuration when the distance between the flankers and the target is greater than about 2λ (when λ is the Gabor wavelength). At lower separation distances, inhibition occurs [1–6]. The studies of Polat and Sagi [1,2] were also the first to report that both facilitation and inhibition phenomena are highly dependent on the target and flankers'

orientations. The highest threshold facilitation is obtained at the fully collinear configuration (Fig. 2 in [2]).

Additional stimulus features, such as the flankers' contrast magnitude, contrast phase, Gabor frequencies, and the size of the Gabor (σ_x, σ_y), also contribute to the lateral interaction effects [1–15].

Several groups have attempted to explain lateral interaction phenomena and proposed computational models [4,9,10,12,16–22]. All of the studies cited above (excluding two studies [9,12]) assumed that two separate mechanisms, facilitation and inhibition, each play an important role in the lateral interaction effect.

None of the models that were previously suggested succeeded in addressing the large variety of stimulus properties that affect the phenomenon (such as global/local orientation, distance, frequency, size, contrast, and phase). These models only attempt to address the outcome of one or two of the flankers' properties [9,10,12,16,17,20,21], or address the effect of the flankers in the presence of a pedestal [18,19,22,23].

Further motivation for a new model includes recent neurophysiological studies (of optical dye imaging [24] and single cell recordings [25]) that showed that the stimulus

configuration of flankers alone (without the presence of a target) can produce a substantial signal in the “target site” (the location between the two flankers), even at large distances from the flankers. Furthermore, the obtained signal is significantly strong for flankers in close proximity (Fig. S3 in [24] supplementary data), and this signal might even be sufficiently strong to generate the perception of a target [24].

Polat and Sagi's psychophysical study [26] might support the above interpretation of neurophysiological results. In their study [26], the subjects performed a Yes/No detection task, in contrast to Polat and Sagi's previous studies in which they used the classical 2AFC method [1]. The results showed a high rate of positive hits, and also a high rate of false-positives, mainly at short distances between the target and flankers (2.5λ). The implication of these results is that at short distances, the observer almost always perceives a target, regardless of whether the target exists or not. One possible interpretation of these results is that the observer might have seen an illusory target, due to the flankers' presence, when a real target was not presented [26].

Due to the perception of the illusory target in the LI phenomenon, the more common 2AFC method might not fully reflect the distinction between facilitation and inhibition mechanisms. The reason for this derives from the fact that the observer is forced to choose one of the two intervals, even though he might perceive the target signal in both intervals. In such a case, the observer might randomly choose one of the two intervals and obtain a high error rate. According to the experiment protocol, this yields an increase in the target contrast. This process causes a threshold elevation that is not derived from a real inhibition mechanism.

In light of the new neurophysiological findings [24,25], and the above interpretation of the threshold elevation in the 2AFC method, we suggest here a new and simple computational model for the lateral interactions effect.

2. MODEL

The model section is divided into three parts. In part 1, there is a schematic description of the observer “decision-making” procedure (Fig. 1), upon which the model is based. In part 2, we suggest a model for the LI mechanism (Fig. 2). In part 3, we elaborate on the two parts of the model in order to predict the psychophysical findings of the LI experiments (Fig. 3).

Part 1—the “observer decision making” (Fig. 1): two images are presented to an observer as part of the 2AFC task.

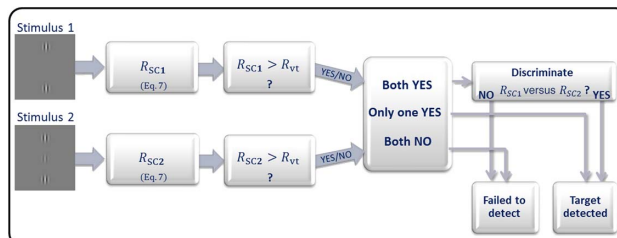


Fig. 1. Model part 1: the “observer decision making.” The inputs are the images of the stimulus with and without a target. The output is the answer whether the target can be detected, and, if so, which interval contains the target.

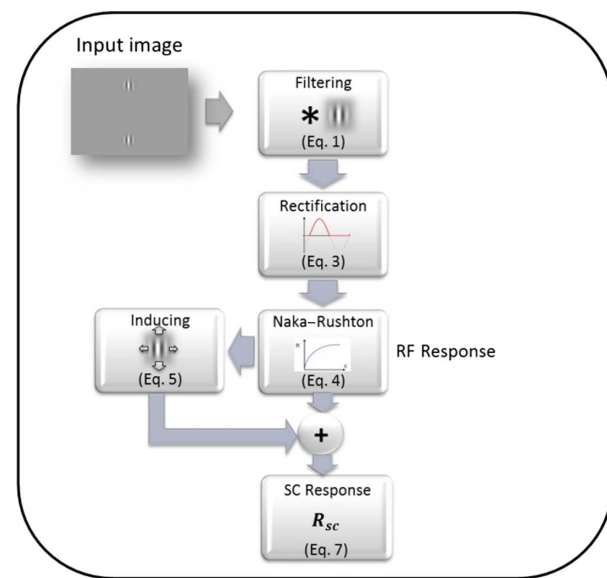


Fig. 2. Model part 2: LI mechanism. The input to the model is an image with any stimulus. The output is the response of the simple cells which have similar spatial properties as the target. The simple cell response includes both the direct RF response (classical RF) and the induced additive signal (from neighboring RFs).

One image includes a target and the other image is presented without a target. The images in both intervals contain the same Gabor flankers. In order to forecast whether the observer can detect the interval with the target, the model examines the simulated response of V1 simple cells (as described in part 2). The cell's response is analyzed separately for the two stimuli of the 2AFC task (Fig. 1).

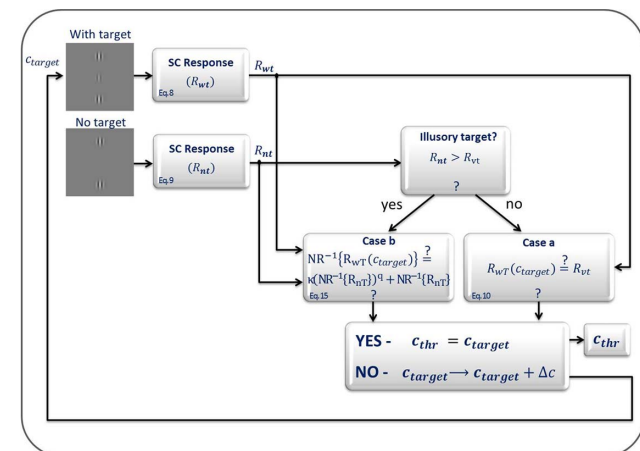


Fig. 3. Model part 3: predicting psychophysical threshold. The input to the model is the flankers' image. If $R_{nT} < R_{vt}$ (no illusory target) then the model Case A is applied, otherwise (i.e., $R_{nT} > R_{vt}$) the model Case B is applied. A different equation is examined, for each case (Case A or Case B), in order to decide whether the target contrast is at detection threshold. The contrast of the target is iteratively increased until the obtained response fulfills the case's equation (Case A or Case B), and yields a YES response (bottom of the flow chart). The contrast which fulfills the equation is the desired target threshold.

Let us first define the term visibility threshold (R_{vt}). The visibility threshold is defined as the minimal receptive field (RF) response which yields an observer perception of a target. For the sake of simplicity of the model, we assume that R_{vt} is the response yielded by a target having a contrast equal to the psychophysical “detection threshold” contrast (C_{vt}).

For each of the two stimuli (with target and without target), the cell’s response may be above or below the visibility threshold (R_{vt}). Altogether there are three possible conditions in reference to R_{vt} : (1) both stimuli responses are above the visibility threshold. In this case the target can be detected only if the observer can discriminate between the two responses (and chooses the interval that obtains the higher response). (2) Only one of the two stimuli (of the 2AFC task) yields a response above the visibility threshold; therefore this stimulus is probably the stimulus with the target. (3) None of the stimuli yield a response above the threshold. In such a case the target cannot be detected.

We assume that when the target cannot be detected or discriminated, the observer probably randomly chooses one of the two stimuli in the 2AFC experiment (i.e., the percentage of correct answers is close to 50%).

Part 2—the LI mechanism: in this part we calculate the simple cell (SC) response in the presence of flankers.

The model assumes that the response of a V1 SC is built upon two components: (1) classical RF response (cRF), and (2) an additive facilitation signal, which is induced by neighboring RFs (nonclassical RF response). The model assumes that the additive signal is induced via long-range horizontal connections (LRHCs) [27,28]. It is possible that the LRHC signal is mediated by a feedback mechanism [21,29–31]. The additive signal is also assumed to be a subthreshold response, i.e., this signal by itself fails to drive the cell (while there is no stimulus in the simple cell RF). The last assumption is in accordance with experimental studies of long-range horizontal connections [30,32]. The additive signal may provide the means for a subthreshold cRF response to elicit an overall superthreshold response. The cRF response includes the flankers’ tails, which invade the “target location” at small flankers’ proximity. Therefore, even at no-target interval a cRF may also have a positive response.

A. Model Formulation

The first stages of the model are aimed to obtain the cRF response map ($R_{RF}(x, y)$). In other words, we calculate the cRF’s responses at every location (x, y) at the input image ($I(x, y)$).

The model assumes a specific distribution of cRFs. The cRF’s centers are separated by distance of λ from each other [33]. Computationally, this sparse image $s(x, y)$ [Eq. (1)] is equal to $I(x, y)$ after it is filtered with a RFs shaped kernel ($G(x, y)$):

$$s(x, y) = \begin{cases} \sum_l \sum_k I(k, l) \cdot G(x - k, y - l) & x, y \text{ at RFs centers} \\ 0 & o.w. \end{cases} \quad (1)$$

We assume that the simple cells’ RFs have a Gabor spatial structure [10,34,35]:

$$G(x, y) = \frac{1}{g} e^{-\frac{(x-x_0)^2+(y-y_0)^2}{\sigma^2}} \cdot \cos\left(\frac{2\pi}{\lambda} \cdot ((x - x_0) \cdot \cos(\theta) + (y - y_0) \cdot \sin(\theta))\right). \quad (2)$$

The frequency ($1/\lambda$) and the orientation (θ) of the spatial filter [Eq. (2)] are determined by the frequency and orientation of the target. σ is the standard deviation of the Gaussian envelope. (x_0, y_0) is the location of the center of the Gabor. g is the normalization factor. In the case that the target is a negative Gabor stimulus (opposite phase target), all the model components remain the same, except that instead of using the kernel $G(x, y)$ in Eq. (1), the kernel $-G(x, y)$ should be used.

The output image is then half-wave rectified, as previously suggested for simple cells’ receptive fields [36]:

$$c(x, y) = \max(s(x, y), 0). \quad (3)$$

The values of $c(x, y)$ [Eq. (3)] are proportional to the contrast of the presented stimulus ($I(x, y)$). In order to better simulate the V1 cRF response we apply a generalization of the Naka–Rushton (NR) equation [37] for V1 cells, as has been suggested previously [38]. This generalized NR transform [Eq. (4)] has been found to be in high agreement with fMRI results for V1 in humans [39]:

$$R_{RF}(x, y) = \text{NR}\{c(x, y)\} = \frac{c(x, y)^{n+m}}{c(x, y)^n + \sigma_{\text{NR}}^n}, \quad (4)$$

where R_{RF} is the response of a cRF unit at location (x, y) . For the sake of simplicity the NR parameters n , m , and σ_{NR} are considered as constants.

Each RF contributes a classical RF response to its SC (cRF). However, the model assumes that this RF may also induce an additive signal to neighboring cells, mainly in the collinear direction. The additive facilitation signal is proportional to the cRF response of the inducing RF.

The induced additive signal has an isotropic distribution with a profile of a 1D Gaussian [Eq. (5)]. The Gaussian weight function reflects the spatial decay of the strength of the induced facilitation as a function of the distance from the inducer. This spatial decay seems to be in agreement with neurophysiological findings (Fig. S3 in [24] supplementary data). Similar spatial function was also assumed by some of the previous LI models [10,17,21]. The additive facilitation (f), as function of the distance, is therefore as follows:

$$f(d, \text{RF}_i) = \begin{cases} 0 & d \leq r_{\text{RF}} \\ a \cdot R_{\text{RF}}^i(x_i, y_i) \cdot e^{-\left(\frac{(d-r_{\text{RF}})}{b}\right)^2} & d > r_{\text{RF}} \end{cases}. \quad (5)$$

RF_i in Eq. (5) represents the RF that induces the facilitation signal ($f(d, \text{RF}_i)$). (x_i, y_i) are the coordinates of the inducing RF (RF_i) and d is the distance from the inducing RF. $R_{\text{RF}}^i(x_i, y_i)$ represents the cRF response [Eq. (4)] of the receptive field RF_i . r_{RF} is the size of the cRF radius. The model parameter a represents the strength level of the induced facilitation. The model parameter b represents the strength of the induced facilitation decay. Note that parameters a , b are orientation-dependent (see Section 3). The induced facilitation is higher for the collinear direction relatively to the

“side by side” direction (direction orthogonal to the collinear direction). This distribution is in agreement with the distribution of the LRHC [31,40].

The assumption that the additive signal is induced only on RFs that are not overlapping with the inducing RF [Eq. (5)] is in agreement with LRHC experimental results [41].

Note that Eq. (5) represents the signal that each RF induces on its neighbors that share its spatial preference (orientation, frequencies, and contrast phase). In other words, the model assumes that lateral interactions only occur within RFs having similar spatial shape. This assumption is supported by LRHC experimental findings [40–44].

All the facilitation signals that are induced to a specific location by its neighboring RFs are summed:

$$F(x, y) = \sum_i f(d^i, R_{RF}^i(x_i, y_i)). \quad (6)$$

F is the sum of the additive facilitation signals at location (x, y) . d^i is the distance between location (x, y) and the location of the (i) neighbor RF (RF_i). A flanker with a spatial frequency/orientation different from that of the target obtains a low R_{RF}^i value. Such RF, therefore, barely contributes to the additive signal [Eq. (6)]. In addition, noncollinear flankers yield a lower $f(d, RF_i)$ value, and contribute less to $F(x, y)$ (relatively to the same flankers at collinear configuration). The model does not require any additional computational processing for accounting the orientation/frequency dependency [apart from this assumption and the usage of Eq. (1) with similar spatial filters].

The total response of a simple cell, $R_{SC}(x, y)$, is the sum of its own cRF response [Eq. (4)] and the additive facilitation signal induced to location (x, y) , by other RFs [Eq. (6)]:

$$R_{SC}(x, y) = R_{RF}(x, y) + F(x, y). \quad (7)$$

Since the model is concerned mainly with the response obtained from the target location (x_t, y_t) , we refer to the SC response at this location ($R_{SC}(x_t, y_t)$). Let us denote the $R_{SC}(x_t, y_t)$ response in the case of an interval with a target as R_{wT} , and in the case of an interval with no target R_{nT} . Similarly, the cRF response at the target location ($R_{RF}(x_t, y_t)$) is marked as $R_{RF|wT}$ and $R_{RF|nT}$ for the interval with and with no target, respectively.

More explicitly, the SC response at the interval with a target is

$$R_{wT} = R_{RF|wT} + F(x_t, y_t). \quad (8)$$

The R_{wT} signal is termed the “compound signal.”

Similarly, at the interval without a target the response is

$$R_{nT} = R_{RF|nT} + F(x_t, y_t). \quad (9)$$

The R_{nT} signal is termed the “bias signal.” Note that even at the interval without a target, for some flankers’ configurations, there might be a real physical stimulus at the “target” location (i.e., $R_{RF|nT} > 0$). This physical stimulus might be the flankers’ tails invading the target site or a pedestal stimulus.

Until now, the purpose of the model was to calculate the response of simple cells in the presence of flankers. This part of the model is generic in the sense that it can be applied to any configuration, with a target stimulus at any contrast (subthreshold or superthreshold), or without a target at all.

Part 3—predicting psychophysical threshold: in the following paragraphs we aim to predict the psychophysical target threshold (c_{thr}) obtained in 2AFC experiments (such as Fig. 3 in [1]). The “observer decision-making” model [part 1 (Fig. 1)] can only determine whether the observer can detect a target with a specific contrast, but it does not determine the target’s threshold. Therefore, our aim is to calculate the psychophysical target threshold. The input to the model (Fig. 3) is the image of flankers as presented to the observer in a psychophysical experiment (with any tested flankers’ configuration). The model output is the target threshold as obtained in the psychophysical experiments.

The model assumes that the observer may perceive a target even when no actual target is presented, i.e., he may see an “illusory target” (model: Case B). An illusory target may be perceived in a stimulus condition in which the bias signal [Eq. (9)] is higher than the visibility threshold R_{vt} . This visibility threshold R_{vt} is the response signal that is required in order to detect a target. R_{vt} therefore equals the response obtained to a target presented alone and having a contrast equal to the detection contrast threshold of this stimulus (c_{vt}). In the case that the bias signal (R_{nT}) is below R_{vt} , the observer will not perceive an “illusory target” (model: Case A).

First, we would like to provide an intuitive description to explain how the model predicts the LI with its different manifestations. Figure 4A illustrates the modeled RF response components that contribute to the LI effect as a function of the distance from the inducing flanker. Figure 4B illustrates the classical LF curve [1] as a function of the flanker-target distance. Note that both x-axes in both figures represent the same distance. Figures 4A and 4B aim to explain the relation between the modeled cells’ response and the obtained psychophysical threshold. The signal obtained due to the presence of the flankers is shown in Fig. 4A. The red curve presents the additive signal ($F(x, y)$), while the blue curve presents the response to both the additive signal and the flanker’s tail R_{nT} . The bias (R_{nT}) signal may be above or below the visibility threshold (the horizontal dotted black line). In the case that R_{nT} is exceeding the visibility threshold, the observer will perceive a target whether the target exists or not (model: Case B). In the case that R_{nT} is below the visibility threshold, the observer will not perceive an illusory target. Now let us assume that a target is also presented. The dashed curves present the total compound signal (R_{wT}) in each distance from the flanker, as would have been obtained if the target was presented at this specific location. The different dashed curves: orange, green and yellow, were obtained for different target contrasts ($c1$, $c2$, and $c3$, respectively).

In the case that R_{wT} is above the visibility threshold, the target is perceived by the observer. The point c (Fig. 4A), which is the crossover point between the orange curve and the R_{vt} line, represents the distance in which the contrast $c1$ is equal to the detection threshold. Therefore, the detection threshold at this distance, i.e., point c' (in Fig. 4B) is equal to the contrast $c1$. Similarly, the crossover point d (green curve, Fig. 4A) corresponds with point d' at Fig. 4B, and therefore the detection contrast at point d' is the contrast $c2$.

At a stimulus configuration where the observer perceives a target, even when the target is not presented (blue curve above

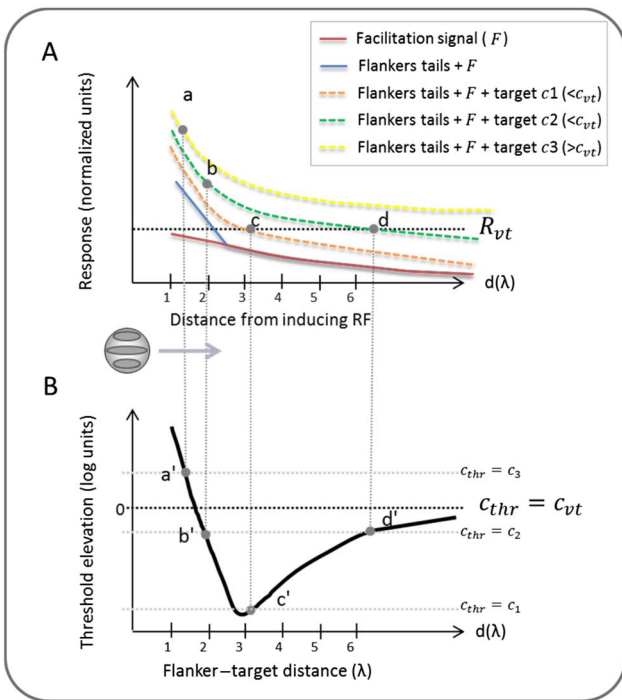


Fig. 4. Example for the relation between the modeled cell’s response and the psychophysical threshold elevation. A, an illustration of the different response components of the modeled RF as function of the distance from the inducing flanker; the additive signal (red curve), the bias signal R_{nT} (blue curve), and the compound signal R_{wT} . The value of the compound signal represents the signal that would have been obtained if a target was presented at that location. It is presented for three different target stimuli. Two target stimuli are with sub-threshold contrasts (orange curve, $c_1 < c_{vt}$; green curve, $c_2 < c_{vt}$), and one target stimulus is with contrast above threshold ($c_3 < c_{vt}$, yellow curve). B, the classical LI threshold elevation Fig. 1. Points a–d in figure A represent the psychophysical target threshold in that proximity from the flankers, and therefore are also represented in figure B (points a’–d’).

black curve), the task that the observer is performing is a discrimination task. The discrimination is between the target and the illusory target. This condition may lead to either threshold elevation (as can be seen in point a, obtained for $c_3 > c_{vt}$) or threshold decrement (point b, $c_2 < c_{vt}$), depending on the strength of the illusory target. In the case that there is no illusory target, the additive signal can lead only to threshold decrement (as can be seen in points c and d for contrast c_1 and c_2 , respectively). Note that the values in Fig. 4A are only for illustration. For the simplicity of the above explanation we referred to the signal originating from the two flankers as if it would have been obtained from one flanker.

There are two distinguishable calculations for the target threshold, depending on whether the observer perceives an illusory target or not. This duality is due to the fact that in each of the two cases (Case A and Case B, below) the observer performs a different task, according to our model.

Case A—no illusory target: the observer does not see an illusory target, i.e., the bias signal is lower than the visibility threshold. In this case, the observer can detect a target when

the compound signal [Eq. (8)] is equal to or higher than the visibility threshold:

$$R_{wT} \geq R_{vt}. \quad (10)$$

Note that we refer to the response (R_{nT}) and not to the delta of response ($R_{wT} - R_{nT}$) that has commonly been applied in previous LI models [4,9,10,12,17,19,22]. The reason for such an approach is that the model assumes that when a bias response (R_{nT}) is below the signal that is required in order to propagate to the next stage (R_{vt}), R_{nT} is considered as being equal to zero. A similar neuronal approach has been suggested previously for similar phenomena, such as the pedestal effect [40–51]. The model suggests that in Case A the above assumption of “neglecting” R_{nT} is valid. The rationale for this is that R_{nT} is approximately equal to the additive facilitation signal ($F(x_p, y_t)$) in the model Case A, but this additive facilitation signal by itself is not sufficiently high to drive the cell [30,32]. R_{nT} , therefore, can be regarded as eliciting zero response.

R_{thr} is defined as the response of the target at the threshold (i.e., with contrast c_{thr}). In the case of a target presented alone, $F(x_t, y_t) = 0$, and therefore Eq. (8) degenerates to $R_{wT} = R_{RF|WT}$ and the threshold equals $R_{thr} = R_{vt}$. In the presence of flankers, however, usually $R_{wT} > R_{RF|WT}$ and therefore $R_{thr} > R_{vt}$. In such a case, a lower target threshold is required in order to perceive a target. Consequently, in Case A, a threshold decrement occurs (i.e., threshold facilitation).

In order to find the target contrast threshold (instead of the response threshold), the response (R_{thr}) can be transformed by the NR inverse function (NR^{-1}) to an equivalent contrast:

$$c = NR^{-1}\{R\}. \quad (11)$$

Equation (11) is the inverse function of the Naka–Rushton equation (Eq. (4)). For the case of parameter $m \neq 0$ (Eq. (4)), $NR^{-1}\{R\}$ can only be calculated numerically.

Note that this transform [Eq. (11)] can only be applied if there is no other physical stimulus input in the target site other than the target itself. In the more general case (for example, while flankers’ tails invade the target location), we calculate numerically the target threshold (c_{thr}), by iteratively changing the contrast of the target until the obtained compound signal (R_{wT}) is equal to the visibility threshold (R_{vt}), thus

$$R_{wT}(c_{thr}) = R_{vt} \quad (12)$$

where $R_{wT}(c_{thr})$ represents the SC response at the interval with target [Eq. (8)], while the target contrast is c_{thr} .

Case B—perceiving illusory target: in this case the bias signal [Eq. (9)] is higher than the visibility threshold. The observer, therefore, perceives a target in both of the 2AFC intervals. The reason for this is that the bias signal is sufficiently high to produce the perception of a target, even in the absence of a physical target. In order to choose the correct interval the observer is required to distinguish the physical target from the illusory target (the bias signal). Hence, instead of a target-detecting task, the observer needs to perform a contrast just-noticeable difference (JND) task.

In order to calculate the psychophysical threshold obtained in this specific case (where an illusory target is perceived), we applied an equation similar to the equation used in the standard contrast discrimination task. In the classical contrast JND task,

there is a physical stimulus (pedestal) at the target site, in both of the 2AFC intervals. A power-law function can be applied in the classical case of a pedestal stimulus [52–54]:

$$c_{\text{thr}} = \kappa \cdot c_p^q. \quad (13)$$

c_{thr} is the increment threshold. c_p is the pedestal contrast. κ , q are model parameters that are dependent on the stimulus spatial properties [54].

Equation (13) can be represented in terms of response values by assigning the NR^{-1} of the response values [Eq. (11)] instead of contrast values:

$$\text{NR}^{-1}\{R_{\text{CS}}(c_{\text{thr}} + c_p)\} = \kappa \cdot (\text{NR}^{-1}\{R_p\})^q + \text{NR}^{-1}\{R_p\}. \quad (14)$$

$R_{\text{CS}}(c_{\text{thr}} + c_p)$ is the response obtained at the interval with both target and pedestal. c_{thr} indicates that this equality is obtained for a target with contrast c_{thr} (i.e., at the detection threshold). R_p is the response for the pedestal stimulus (i.e., the interval with no target).

In the classical LI configuration [1] there is no pedestal stimulus in the target site. However, R_{nT} can be considered analogous to a pedestal stimulus. We modify Eq. (14) to apply to the case of LI:

$$\text{NR}^{-1}\{R_{\text{wT}}(c_{\text{thr}})\} = \kappa \cdot (\text{NR}^{-1}\{R_{\text{nT}}\})^q + \text{NR}^{-1}\{R_{\text{nT}}\}. \quad (15)$$

In the model simulations the target contrast is iteratively changed in order to find the contrast (c_{thr}) that fulfills Eq. (15). In many cases, the values of R_{nT} are such that they yield a higher target threshold (c_{thr}) than the threshold (c_{vt}) for target alone (i.e., $c_{\text{thr}} > c_{\text{vt}}$). In other words, threshold elevation is obtained. Such threshold elevation is not due to an inhibition mechanism, but rather results from the presence of the illusory target. We term this threshold elevation “pseudo inhibition.”

We have divided the model into two cases, depending on whether the observer perceives an illusory target (Case B) or not (Case A). This was done for the sake of simplicity. However, it is more psychophysically accurate to test the statistical probability that the observer will perceive an illusory target at a certain bias signal. When the bias signal is significantly lower than the visibility threshold, the observer most likely will not perceive the illusory target (i.e., Case A). When a bias signal is significantly higher than the visibility threshold, an observer most likely will always perceive an illusory target (i.e., Case B). When a bias is close to the visibility threshold (R_{vt}) the threshold value will have an intermediate value between the above two cases. Since the statistical analysis is more complicated and requires unknown statistical distributions, we chose to use the above simplification. The statistical solution cannot dramatically change the final outcome. It may affect at most only one point in the presented figures (i.e., the point where the bias signal is in proximity to the visibility threshold).

3. METHODS

We synthesized different flankers’ configurations as input images to the computational model. The model input is these images only, without any additional information regarding the flankers. The parameters (λ) and (θ) of the Gabor kernel [Eq. (2)] are identical to the parameters of the target to which

the threshold is calculated. We assumed that the size of the RF is constant and equal to 2λ (RF radius $r_{\text{RF}} = \lambda$) [55]. The Gaussian envelope parameter (σ) of the RF was assumed to be equal to λ (13.3 cyc/deg or 6.67 cyc/deg).

The facilitation strength parameter [α in Eq. (3)] and facilitation decay parameter [b in Eq. (3)] were adjusted in order to obtain a threshold decrement that is similar to the psychophysical threshold decrement (Fig. 2 in [1]; Fig. 2 in [2]).

For the sake of simplicity of the model, we accounted only for the RF that yields the highest response with the specific target, even though in a real psychophysical system additional RFs can play a role in the final outcome.

In most of the presented figures (see Section 4), the input images consisted of Gabor patterns [Eq. (2)] with $\sigma = \lambda$, unless noted otherwise. We choose to apply stimulus parameters at the curves of the threshold elevation as a function of distance, with the same values as those reported by Polat and Sagi [1]. The model obtained good results using the same facilitation decay parameter [b , Eq. (5)] for both frequencies (high and medial). We assumed therefore, that both frequencies have the same value of $b = 5.5$ (normalized value, model). The simulations are applied with the same facilitation strength parameter value [α , Eq. (5)] for the collinear directions and for the “side by side” directions. The decay parameter for the “side by side” direction [b , Eq. (5)] is assumed to be equal to a half of the decay parameter for the collinear direction ($b_{\text{sidewise}} = 2.25$), contributing a stronger decay with distance, as obtained psychophysically. Such distribution is similar to what is found for the LRHC collinear dependency [40].

If not noted otherwise, in all plotted figures $m = 0.4$, $n = 2$, $c_{50} = 15\%$, $\sigma = \lambda$, $b = 5.5$, $b_{\text{sidewise}} = 2.25$. For the medial frequency $\alpha = 0.01$, $c_{\text{vt}} = 5\%$, and for the high frequency $\alpha = 0.12$, $c_{\text{vt}} = 15\%$.

4. RESULTS

We have tested the model predictions for different stimuli configurations that have been established in the LI studies.

A. Target–Flanker Distance

Figure 5 presents the model prediction for the threshold elevation as a function of the target–flanker distance, with different NR parameters (exponents n , m , and half-saturation constant c_{50}). A, $m = 0.4$, $\sigma_{\text{NR}} = 15\%$. B, $n = 2$, $m = 0.4$. C, classical Naka–Rushton equation ($m = 0$), $n = 2$. The model parameter α is determined according to psychophysical results [2] (Methods).

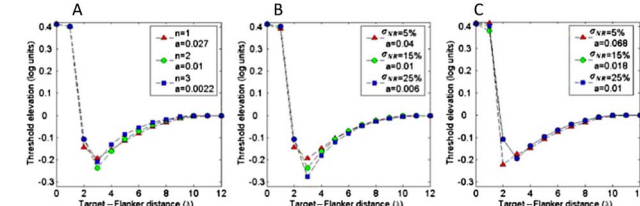


Fig. 5. Model predictions of the classical LI effect: the threshold elevation as a function of the target–flanker distance. The threshold is normalized to the target-alone threshold (5%) obtained in psychophysical experiments [2]. A–C present the model’s prediction for different NR parameters (exponent n , m , and half-saturation constant c_{50}). A, $m = 0.4$, $\sigma_{\text{NR}} = 15\%$. B, $n = 2$, $m = 0.4$. C, classical Naka–Rushton equation ($m = 0$), $n = 2$. The model parameter α is determined according to psychophysical results [2] (Methods).

constant σ_{NR}). The obtained curves resemble the experimental results [1–6].

Figure 5 demonstrates the immunity of the model's results to different NR parameters to account for the large variety of NR parameters in the experimental literature [39,51,56–63]. Although in all cases the threshold for the target alone is identical ($c_{vt} = 5\%$), the derived facilitation strength (a) is highly affected by the NR parameters. In other words, in order to obtain in the simulation the same curve for different NR parameters, the model parameter a needs to be changed according to the NR parameters.

B. Spatial Frequencies

Figure 6 shows the simulation results for the two tested spatial frequencies 13.3 cyc/deg ($\lambda = 0.075^\circ$) and 6.67 cyc/deg ($\lambda = 0.15^\circ$). The obtained results highly resemble the experimental results (Fig. 3 in [1]). Note that the threshold for the target presented alone (c_{vt}) is determined to be 5% for the medial frequency and 15% for the high frequency, in accordance with psychophysical experiments [1], whereas c_{vt} for both frequencies have different values, the value obtained by the model for the visibility threshold (R_{vt}) is highly divergent between the two frequencies. A possible reason for this change in R_{vt} is that the model is using the same NR parameters for both frequencies. In additional simulation in which NR parameter σ_{NR} of the medial frequency was chosen to be lower than σ_{NR} of the high frequency, the diversity in the values of R_{vt} between both frequencies was reduced. This difference in σ_{NR} follows the trend that has been observed experimentally [39,64]. In any case, the different curves obtained for different σ_{NR} values are almost identical (Fig. 5). Therefore, in terms of comparison between the model results (Fig. 6) and psychophysical results (Fig. 3 in [1]), it makes no difference whether or not we choose identical values of σ_{NR} for the two frequencies.

The differences in the visibility threshold may explain the high difference in the amount of facilitation (a), which is required for the high and the medial frequencies ($a = 0.12$ and $a = 0.01$, respectively). In the simulation in which the NR

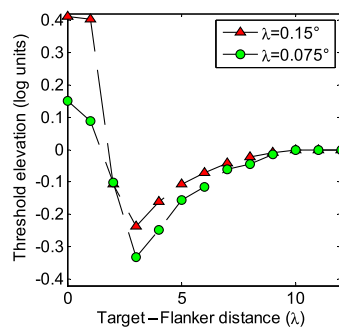


Fig. 6. Model's results of the threshold elevation as a function of target–flanker distance, for two different spatial frequencies: 13.3 cyc/deg (i.e., $\lambda = 0.075^\circ$) and 6.67 cyc/deg (i.e., $\lambda = 0.15^\circ$). The threshold for the target presented alone is 5% for the medial frequency (6.67 cyc/deg) and 15% for the high frequency (13.3 cyc/deg) [1]. The facilitation strength parameter is $a = 0.01$ for the medial frequency, and $a = 0.12$ for the high frequency.

parameters yield similar R_{vt} values for both frequencies, the difference between the values of a was significantly lower.

Both frequencies obtain different threshold elevation at close proximity. The main reason for this result is the fact that the presented threshold elevation is normalized to the threshold for target alone. The threshold for target alone is different between the medial and the high frequencies (5% and 15%, respectively).

We simulated only two frequencies. However, if one would assume the exact same parameters (a, b, c_{vt}) for high and medial frequencies, then the figures that would be obtained would be identical to what was presented here for the medial frequency. The assumption that the parameters should be similar is a reasonable assumption, since lower frequencies indeed obtain similar c_{vt} values as 6.67 cyc/deg frequency [1]. The psychophysical results (Fig. 3 in [1]) also obtain similar curves for 6.67, 1.5, and 3.34 cyc/deg frequencies. The small variation in the psychophysical result can be caused by slightly different facilitation strength parameters (Fig. 7A).

C. Facilitation Strength Parameter

Figure 7 shows the effect of the facilitation strength parameter [a , Eq. (5)] on the classical experimental curve that shows the dependence of the threshold elevation on the flankers' distance. The simulations indicated that for lower values of the parameter a (e.g., $a = 0.09$), the strongest threshold decrement is obtained at a distance of 2λ (Fig. 7B). At higher facilitation strength ($a \geq 0.1$) the highest threshold decrement is obtained at a distance of 3λ . The model prediction for $a = 0.09$ is in agreement with the results of Polat and Sagi [2] (triangles curve, Fig. 1). The model predictions for $a \geq 0.1$ are in agreement with the results of Polat and Sagi [1] (triangles curve, Fig. 1). Both of the figures presented by Polat and Sagi were obtained in essentially the same experimental procedures, but among two different observers. The implication of the above results may suggest that the differences between the curves might originate from differences in the strength of facilitation among different observers. However, slightly different NR parameters (for different observers) can also predict the observed differences between the two observers.

It may seem surprising that the weakest facilitation value causes the highest threshold decrement (Figs. 7A and 7B) at

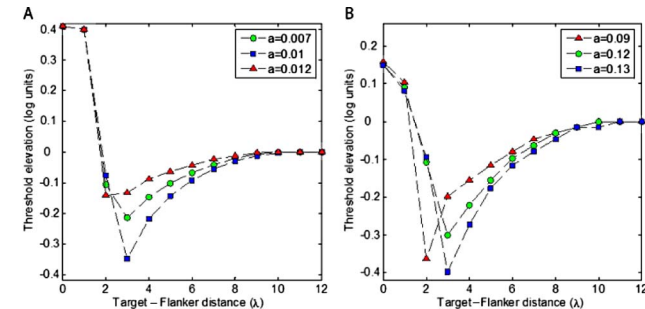


Fig. 7. Effect of the facilitation strength parameter (a) on the simulated threshold elevation as a function of distance for two Gabors' parameters: A, high Gabor spatial frequency (13.3 cyc/deg). B, medial frequency (6.67 cyc/deg).

a distance of 2λ . The reason for this is that at a distance of 2λ , an illusory target might be perceived. In such a case the task can be regarded as a JND task (model: Case B), and therefore a higher facilitation causes a stronger illusory target, and may cause a higher threshold elevation.

D. Target–Flankers Orientation

Figure 8 presents the effect of the target–flankers orientation on the LI threshold elevation/decrement. In order to enable us to compare the model’s predictions with the psychophysical results (Figs. 2 and 4 in [1]), the presented model’s predictions (Fig. 8) were simulated with high-frequency stimuli (13.3 cyc/deg). Simulations with medial-frequency stimuli exhibit results that are similar to the results obtained at high spatial frequency (Fig. 8).

Figure 8B demonstrates the high dependency of the LI in the global target–flankers orientation. We simulated the three types of global target–flankers orientations: collinear, “side by side,” and diagonal [2]. The model predicts that the collinear configuration exhibits the highest threshold decrement, while the “side by side” stimulus configuration exhibits lower threshold decrement. This threshold decrement decreases strongly over the target–flankers distance. These results highly resemble the results obtained by Polat and Sagi [2].

Our model predicts a very small threshold decrement in the diagonal configuration at a 3λ distance (Fig. 8B). This trend of

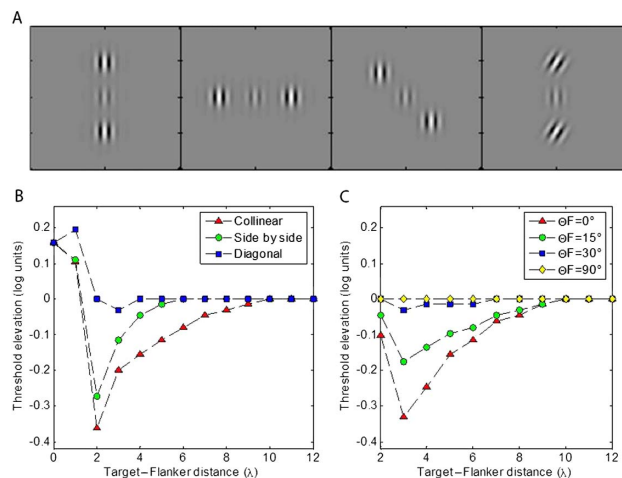


Fig. 8. Model prediction of the lateral interactions’ dependency on the target–flankers orientation. A, an example of the tested configurations (from left to right): collinear configuration, “side by side” configuration, diagonal configuration, and a test configuration containing flankers with local orientation of 30° (all configurations are presented with strong target and flankers contrast for illustration purposes). B, model predictions of the three different global orientations: collinear, “side by side,” and diagonal. C, model predictions of different local orientations: Flankers’ orientations of 0° , 15° , 30° , 90° (while target orientation is 0°). Both figures are plotted for high-frequency stimuli, in order to enable comparisons with the psychophysical results (Figs. 2 and 4 in [1]). Note that for Fig. 5A we chose the weaker facilitation strength parameter ($a = 0.09$, for all configurations). We chose this facilitation parameter in order to enable the obtainment of the strongest facilitation at 2λ for collinear configuration, as obtained by the observer in the comparable psychophysical experiment of Polat and Sagi [1]. In Fig. 5C we used the default value ($a = 0.12$).

results is in agreement with the results of Polat and Sagi [2], though they obtained a slightly stronger threshold decrement. According to our model the threshold elevation obtained at a 1λ distance in the diagonal configuration (Fig. 8B) is not due to “pseudoinhibition.” Rather, the threshold elevation is due to the fact that at this distance the target and the Gabor flankers are basically in destructive interference (their overlapping areas have opposite contrast phase). In such a case, therefore, a higher target threshold is required in order to cause the response to be equal to the response visibility threshold (R_{vt}).

Figure 8C demonstrates the high dependency of the LI curves on the orientation of the flankers (local orientation). We simulated four different flankers’ orientations (0° , 15° , 30° , and 90°), while target orientation was kept constant at 0° (vertical aligned Gabor). The collinear configuration (same orientation for target and flankers) obtains the highest threshold decrement. The 15° orientation of the flankers shows slightly smaller, yet high threshold decrement. Higher orientation differences (above 30°) lead to insignificant threshold decrement. This trend of our results is similar to the psychophysical results (Fig. 4 in [2]).

E. Flankers’ Size

Figure 9 demonstrates the effect of the flankers’ height (σ_y) on the threshold elevation. The model predicts that a higher flanker, at the range of heights ($\sigma_y = 0$ – 1.5λ), leads to a stronger induced facilitation, and therefore stronger threshold decrement. When the bias signal becomes sufficiently strong ($\sigma_y = 1.5$ – 2λ), it can lead to “pseudoinhibition,” and therefore to threshold elevation. Our results are in agreement with the results obtained by Nugent and his colleagues [13,14]. The model results for a normal facilitation strength ($a = 0.01$ – 0.012) highly resemble the psychophysical results obtained by observers AN and RW (Fig. 6 in [13]). The model results for higher facilitation strength (Fig. 8, $a = 0.014$) highly resemble the results for observer BH (Fig. 6 in [13]). Alternatively, computing the model with weaker facilitation decay [higher value for parameter b , Eq. (5)], lower threshold for target alone (c_{vt}), or a different NR function’s parameters, could also predict stronger threshold elevation at $\sigma_y = 1.5\lambda$.

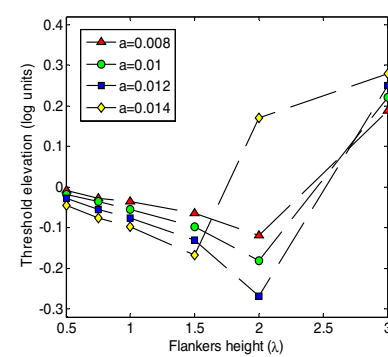


Fig. 9. Model predictions of the threshold elevation as a function of the flankers’ height (σ_y), for a target–flankers distance of 6λ . The figure is plotted for medial frequency (high frequency obtained similar results). We used four different facilitation strength parameters ($a = 0.008$, 0.010 , 0.012 , and 0.014).

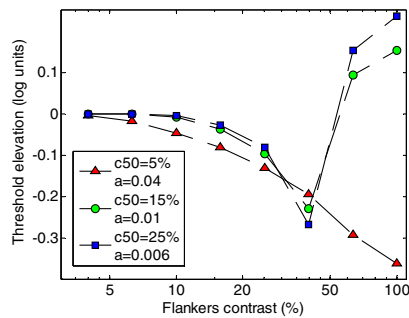


Fig. 10. Model predictions of the threshold elevation as a function of the flankers' contrast, for a target–flankers distance of 3λ . The figure is plotted for medial frequency (the high frequency obtained a similar trend of results).

F. Flankers' Contrast

Figure 10 presents the model predictions for threshold elevation as a function of the flankers' contrast. The induced facilitation signal can be high enough to produce “pseudoinhibition” at high flankers' contrast, for some NR parameters (for example, blue and green curves in Fig. 10). In these cases a high threshold elevation occurs. Psychophysical results also show that at high flankers' contrast the threshold elevation increases [10,12]. Though we obtained a similar trend, it seems that the threshold elevation obtained experimentally is more restrained than the elevation obtained by the model. This digression between the model's predictions and the experimental results can originate from weak inhibition caused by other mechanisms. This weak inhibition may no longer be negligible at very high contrast flankers (see Section 5.F).

G. Opposite Phase

Figure 11 (red curve) presents the model prediction for flankers having opposite phase to each other (i.e., only one flanker has the same contrast phase as the target). The model yields a much smaller threshold decrement for the configuration of flankers having opposite phases, in comparison to the same phase colinear configuration. The explanation for this behavior is that the model assumes that facilitation is induced only for same phase neighboring RFs (model). Under this assumption only

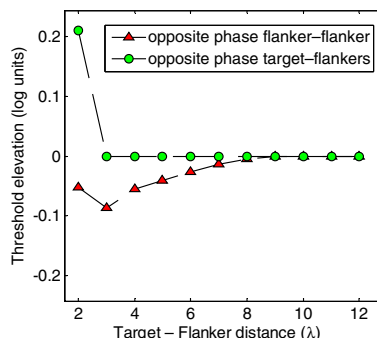


Fig. 11. Model predictions for the dependency of LI on the contrast phase. The green curve presents the condition where the flankers have an opposite phase to the target. The red curve presents flankers having opposite phase (only one flanker has opposite phase to the target).

one flanker contributes induced facilitation to the target site, and therefore an overall smaller facilitation signal is obtained (for distances of $d \geq 3\lambda$). This result is in agreement with the psychophysical result (Fig. 12 in [65]).

The model predicts the absence of the LI effect for a configuration in which both flankers have a phase that is opposite to the target (green curve, Fig. 11). The threshold elevation at the 2λ distance is obtained due to destructive interference. The overlapping flankers have opposite contrast phase, and therefore decrease the signal at the target site (threshold elevation).

5. DISCUSSION

This is the first time that a robust computational model has been suggested for the different manifestations of the LI effect. Our model assumes that the LI phenomenon, which includes both facilitation and inhibition aspects [1], can be explained mainly by one simple mechanism: a positive additive facilitation signal. The additive signal is induced by the flankers on the target site, even in the absence of a real target. The model predicts psychophysical results of various manipulations of the flankers—target distance, position, contrast, orientation, size, spatialphase, and more (Figs. 5–11).

Our model is based mainly on standard building blocks, such as modeling RFs with a Gabor kernel [Eqs. (1) and (2)] or applying the generalized Naka–Rushton equation [Eq. (4)]. However, our model has two main deviations from the common approach. First, our model is based upon nonclassical interpretation of the threshold elevation experimental result. The threshold elevation in our model is due to a strong additive facilitatory signal, while previous studies attribute it to an inhibitory mechanism [10,16,17,19–23]. Second, the threshold decrement in our model is also obtained directly from the additive signal. This is obtained without the need for an additional, nonclassical, accelerating function, as performed in previous studies [10,17,19,22]. Such a simple approach was applicable due to embedding a “response threshold” (R_{vt}) in the model.

In this paper, we present only model simulations that predict the effect of the flankers on the detection threshold. However, the model aims to predict the LI effect also for target stimuli, above threshold or below threshold. The model is built in a generic way such that the equations [Eqs. (1)–(9)] are not limited to predicting the detection threshold. We restricted the model's simulations to measures which have been tested experimentally as well, and enable validation of the model's predictions. In order to test whether the outcome of Eq. (7) is correct, more LI neurophysiological experimental findings are required.

A. Problematic Stimulus Paradigm (2AFC Paradigm)

A stimulus paradigm which forces the observer to choose one of two alternative choices (such as the 2AFC paradigm) might lead to ambiguous results. The threshold elevation can theoretically originate from one of the two opposite mechanisms: (1) a real inhibition, or (2) a significantly high additive facilitation signal. In the first condition (real inhibitory mechanism), the decrease in the target response (due to inhibition) may lead to threshold elevation. In the second condition, in the presence of a high additive facilitation signal, the additive signal (plus the response

of the flankers' tails) may be sufficiently strong to produce an illusory target. In this case, the observer perceives a target in both of the 2AFC stimuli presentations. In a condition of a target with low contrast, the observer probably cannot distinguish which interval contains a target. The reason for this is that both the illusory target and the real target are almost equal candidates for being the target. The observer, therefore, will most likely randomly choose one of the two intervals. Such a probable condition would lead to threshold elevation ("pseudoinhibition"). This threshold elevation (of condition 2) might be misinterpreted as real inhibition (condition 1).

Polat and Sagi [26] suggested a method that can help overcome the ambiguous results of the 2AFC paradigm. In their paper, the additive facilitation signal is termed "filling in" (or "illusory perception"). In order to test whether an additive signal exists, they used a Yes/No procedure, in addition to the standard 2AFC paradigm. Due to their approach, if the Yes/No experimental result has a high false-positive and high hit rate, then such a result supports the existence of an additive facilitation signal (for example, Fig. 2a in [26]). Note, however, that this approach can also introduce a new difficulty. Polat and Sagi reported that in some testing conditions "observers could correct for false-positive responses by adjusting their response criterion" [26]. Therefore, in order to test whether an additive signal mechanism exists, it is important that the experimental conditions do not permit a significant adjustment in the decision-making criteria.

B. SC Response Versus Delta of Response

In order to determine whether the interval with a target can be detected (model, Case A) our model refers to the value of the compound SC response [R_{wT} , Eq. (8)] and not the delta of response ($R_{wT} - R_{nT}$; [66]). Green and Swets [66] claimed that ignoring R_{nT} is legitimate only in the case where the interval without a target contains nothing but noise. We believe that our model's approach does not contradict Green and Swets' approach [66]. This is because the additive facilitation signal alone is not sufficiently high to drive the cell [30,32]. As R_{nT} approximately equals the additive facilitation signal ($F(x_t, y_t)$) in Case A, R_{nT} can be regarded as eliciting zero response.

One could ask whether Case A in our model can be more general and refer also to pedestal experiments where the real stimulus (pedestal) is with subthreshold contrast, and not only refers to the suggested additive signal [Case A; Eq. (5)]. We found that the same approach has been suggested previously in reference to the pedestal effect [40–51] and also for discriminating the direction of drifting gratings [51]. Foley and Legge [67] showed that only when such a pedestal model embeds an internal noise, this model succeeds to correctly predict experimental data. Even though we believe that their approach is more accurate, it is not expected to change our model's results, which did not refer to statistical measures and only predicts the average detection threshold (Figs. 5–11).

C. Mechanisms/Undelaying the LI Effect

Previous studies suggested that the LI mediated via LRHCs [2,7,15,18]. Our model also relies on this assumption. Our model assumes that the additive signal is originated from the

LRHC; however, the model does not contradict the possibility that an additional mechanism also mediates the additive signal, as suggested in the literature [21,29,30]. Grossberg and Raizada [21], for example, suggested that the feedback interactions are needed in order to selectively attend to the signal originated by the LRHC, and also included such a component in their model for perceptual grouping and object-based attention in the primary visual cortex.

D. Opposite Phase

There is no consensus in the literature regarding the issue of whether the LI effect is phase-dependent or not. This property is manifested by obtaining the same or different responses to flankers with opposite phase to the target (compared to the classical same-phase configuration). Our model predicts that the threshold decrement for the same-sign target flankers is higher than for a configuration where one of the flankers, or both flankers, have an opposite phase to the target. This phase dependency is due to the relevant model assumption (model). This prediction is in agreement with the large majority of LI results that show phase dependency [5,9–12,65,68].

Several studies found a small degree of facilitation for an opposite phase target–flankers configuration [9,11,68]. We wonder if this moderate facilitation is derived from the same mechanism of the classical LI effect, in light of the fact that similar (moderate) facilitation has also been obtained for configurations of perpendicular flankers or cues [68,69].

E. Previous Computational Models

The classical interpretation of the threshold inhibition that was obtained experimentally at flankers with close proximity [1] is that the flankers induce strong inhibition in the target site. Based on this interpretation of results, most of the computational studies suggested models built from two independent mechanisms: inhibition and facilitation [10,16,17,19–23]. The inhibition has a strong and narrow weight function, while the facilitation has a broad and weaker weight function (for example, Fig. 9 in [10]).

Our model, on the other hand, relies on a different interpretation of the observed threshold elevation. We assumed that the threshold elevation is mostly due to "pseudoinhibition" (see Section 5.B), while the actual inhibition was assumed to have only a minor effect on the perceived threshold elevation (at least in the classical paradigm of a target and two flankers).

Our model assumed a subthreshold additive facilitatory signal similarly to what have been previously suggested by other studies [10,17,21]. However, we assume that this mechanism is the only mechanism that plays a major role in the LI effect, and that a strong inhibitory mechanism is not needed in order to predict the psychophysical results (Figs. 5–11).

Solomon *et al.* [9] also proposed a model that assumes that an inhibition mechanism is not required. Solomon *et al.* [9] suggested that large receptive fields might be sensitive to both a target and flankers, even when they are separated by a distance of 6λ . Acting on such an assumption they attempted to fit a transducer model to the findings of Polat and Sagi [1] and to their own findings. Their model predicts threshold elevation for spatially adjacent flankers and threshold decrement

(facilitation) for distant flankers. However, in addition to the fact that, as far as we know, there is no evidence for such a large RF in the fovea, their model did not predict long-range threshold decrement for distances longer than 4λ .

In a later work [12], Solomon and Morgan further expanded their 1999 model. Their expanded model succeeds fairly well to predict collinear lateral facilitation and also successfully predicts the lack of facilitation in the opposite phase condition. In both configurations of same and opposite phase, the model's simulations were applied only for a distance of 3λ , and there are no predictions of this model for the classical figure of Polat and Sagi [1]. Furthermore, the model does not predict the obtained facilitation in the condition of side by side configuration (Fig. 7 in [12]).

Other than our nonclassical interpretation of the experimental threshold elevation, an additional major difference between our model's approach and previous models' approaches is in regards to the assumed mechanism that leads to threshold decrement. Previous models [4,9,10,12,17,19,22] assumed that the responses for the two stimuli conditions (with target and without target) should always be subtracted and the delta of response should be referred to (see Section 5.C). Within a model which refers to the delta of response, an additive induced signal alone cannot lead to threshold decrement as it is eliminated by the subtraction. Consequently, previous studies had to suggest models embedding a more complex accelerating function instead of the well-established Naka–Rushton equation [10,17,19,22]. Our model assumes that the additive induced signal is the only mechanism responsible for the threshold decrement, due to the fact that this bias signal allows a subthreshold target to become visible (model: Case A). This analysis is relevant only under the assumption that the bias signal (in Case A) should not be eliminated.

We would like to note that some of the previous models that aimed to address the LI phenomenon actually refer to experimental data that is not necessarily derived from the mechanism of LI. For example, the model of Cannon and Fullenkamp [70] attempted to predict experimental results obtained with a stimulus configuration which is not the classical LI. We referred to their stimulus paradigm as evoking a different mechanism called surround suppression (see Section 5.G). Grossberg and Raizada [21], for example, predicted the neurophysiological data which referred to simple and complex cells' responses as a function of target contrast. The fact that complex cells also show the effect seems to us problematic in referring this data to the LI effect, since the complex receptive fields are not sensitive to the polarity of the stimulus while the LI effect has been found to be sensitive to the stimulus polarity [5,9–12,65,68].

F. Additional Influencing Processes

Even though we show that the induced facilitation signal can govern the LI phenomenon, as always, additional cortical mechanisms are also involved in order to produce the final output (psychophysical results). For example, the contrast-contrast effect (also known as surround suppression) [16,70,71,72] and attention aspects [69,73].

The contrast-contrast phenomenon is classically examined in the stimulus condition of an iso-oriented surrounding disk

[70,71,74]. Several previous studies assumed that the effect of the contrast-contrast phenomenon and the effect of LI share the same mechanism [75]. This approach is inconsistent with the fact that the LI phenomenon and the contrast-contrast phenomenon are manifested by different temporal and spatial properties and are attributed to different mechanisms [15,71,74–78]. In particular, the two effects have different temporal properties: LI is much slower than the contrast-contrast effect [15,76–78]. Cass and Spehar [15] psychophysically discovered that the propagation velocity of the LI effect is approximately 0.10–0.23 m/s. They concluded that the lateral interactions closely corresponded with long-range horizontal connections. Kilpelainen *et al.* [76], on the other hand, psychophysically tested the dynamic of the contrast-contrast phenomenon and found that the propagation velocity was approximately 1 m/s. They concluded that "such a short delay of suppression is consistent with a neural implementation based on feedforward–feedback connections, but not with horizontal connections." The contrast-contrast neurophysiological experiments of Bair *et al.* [79] also support the results of Kilpelainen *et al.* [76], namely that the velocity is about 1 m/s.

The spatial aspects of the two phenomena, LI and contrast-contrast, appear to show different spatial requirements. The effect of the contrast-contrast phenomenon does not require collinearity of the target and its mask [71,74,75], while in the LI phenomenon this property has a dramatic effect on the obtained results [2]. Furthermore, it has been shown that the contrast-contrast facilitation (but not inhibition) is not orientation specific. This implies that the same facilitation is obtained for orthogonal and same target–mask orientation [71]. LI, on the other hand, is clearly orientation-specific [2].

One additional major difference between these phenomena is that the LI effect requires that the target and its flankers be at the same phase polarity [5,9,11,12,68], while in the contrast-contrast effect the phase of the target and its surround grating stimulus is not relevant [71,75].

We believe that the role of the contrast-contrast mechanism is to enhance the texture difference of a stimulus from its surrounding texture background. The role of LI, on the other hand, is to complete low-texture areas based on the similarity to surrounding stimuli. It is reasonable to assume that different mechanisms always coexist in the visual system though they may contradict each other in specific stimulus conditions, as might happen with the LI and contrast-contrast phenomena.

Several experimental studies used stimuli that could be related to both types of mechanisms. One such example is stimulus configuration with four or more flankers [12,17,74]. In such a stimulus configuration both phenomena can have a major effect on the perceived target contrast.

In conclusion, in this study we have demonstrated how the existence of a positive additive signal induced by the flankers can solely explain the classical LI effects. This additive mechanism predicts both the threshold decrement (facilitation) and elevation ("inhibition") obtained experimentally. The above fundamental assumption, that the additive mechanism is responsible for both aspects of the LI phenomenon, enables us to suggest a simple but inclusive computational model for the LI phenomenon. The proposed model succeeds to correctly

predict the basic LI effect as a function of distance (Fig. 2 in [1]). It also correctly predicts additional experimental results, such as the effect of the flankers' global/local orientation, frequency, size (sigma), contrast, and phase.

REFERENCES

- U. Polat and D. Sagi, "Lateral interactions between spatial channels: suppression and facilitation revealed by lateral masking experiments," *Vis. Res.* **33**, 993–999 (1993).
- U. Polat and D. Sagi, "The architecture of perceptual spatial interactions," *Vis. Res.* **34**, 73–78 (1994).
- R. G. Giorgi, G. P. Soong, R. L. Woods, and E. Peli, "Facilitation of contrast detection in near-peripheral vision," *Vis. Res.* **44**, 3193–3202 (2004).
- C. C. Chen and C. W. Tyler, "Excitatory and inhibitory interaction fields of flankers revealed by contrast-masking functions," *J. Vis.* **8**(4):10, 1–14 (2008).
- C. B. Williams and R. F. Hess, "Relationship between facilitation at threshold and suprathreshold contour integration," *J. Opt. Soc. Am. A* **15**, 2046–2051 (1998).
- R. L. Woods, A. K. Nugent, and E. Peli, "Lateral interactions: size does matter," *Vis. Res.* **42**, 733–745 (2002).
- U. Polat, "Functional architecture of long-range perceptual interactions," *Spat. Vis.* **12**, 143–162 (1999).
- U. Polat and D. Sagi, "Spatial interactions in human vision: from near to far via experience-dependent cascades of connections," *Proc. Natl. Acad. Sci. USA* **91**, 1206–1209 (1994).
- J. A. Solomon, A. B. Watson, and M. J. Morgan, "Transducer model produces facilitation from opposite-sign flanks," *Vis. Res.* **39**, 987–992 (1999).
- B. Zenger and D. Sagi, "Isolating excitatory and inhibitory nonlinear spatial interactions involved in contrast detection*," *Vis. Res.* **36**, 2497–2513 (1996).
- P. C. Huang, K. T. Mullen, and R. F. Hess, "Collinear facilitation in color vision," *J. Vis.* **7**(11):6, 1–14 (2007).
- J. A. Solomon and M. J. Morgan, "Facilitation from collinear flanks is cancelled by non-collinear flanks," *Vis. Res.* **40**, 279–286 (2000).
- A. K. Nugent, R. L. Woods, and E. Peli, "Flanker size affects visual lateral interactions," in *Association of Research Vision Ophthalmology 2002 Annual Meeting, CD-ROM* (2002), Vol. **4718**.
- A. K. Nugent, R. L. Woods, and E. Peli, "Lateral interactions: two effects of flanker size," *Invest. Ophthalmol. Visual Sci.* (2002).
- J. R. Cass and B. Spehar, "Dynamics of collinear contrast facilitation are consistent with long-range horizontal striate transmission," *Vis. Res.* **45**, 2728–2739 (2005).
- M. W. Cannon and S. C. Fullenkamp, "A model for inhibitory lateral interaction effects in perceived contrast," *Vis. Res.* **36**, 1115–1125 (1996).
- Y. Adini, D. Sagi, and M. Tsodyks, "Excitatory-inhibitory network in the visual cortex: psychophysical evidence," *Proc. Natl. Acad. Sci. USA* **94**, 10426–10431 (1997).
- C. C. Chen and C. W. Tyler, "Lateral sensitivity modulation explains the flanker effect in contrast discrimination," *Proc. R. Soc. London Ser. A* **268**, 509–516 (2001).
- C. C. Chen and C. W. Tyler, "Lateral modulation of contrast discrimination: flanker orientation effects," *J. Vis.* **2**(6):2, 520–530 (2002).
- K. Mizobe, U. Polat, M. W. Pettet, and T. Kasamatsu, "Facilitation and suppression of single striate-cell activity by spatially discrete pattern stimuli presented beyond the receptive field," *Vis. Neurosci.* **18**, 377–391 (2001).
- S. Grossberg and R. D. Raizada, "Contrast-sensitive perceptual grouping and object-based attention in the laminar circuits of primary visual cortex," *Vis. Res.* **40**, 1413–1432 (2000).
- C. C. Wu and C. C. Chen, "Distinguishing lateral interaction from uncertainty reduction in collinear flanker effect on contrast discrimination," *J. Vis.* **10**(3):8, 1–14 (2010).
- B. Zenger-Landolt and C. Koch, "Flanker effects in peripheral contrast discrimination-psychophysics and modeling," *Vis. Res.* **41**, 3663–3675 (2001).
- E. Meirovitz, I. Ayzenshtat, Y. S. Bonneh, R. Itzhack, U. Werner-Reiss, and H. Slovin, "Population response to contextual influences in the primary visual cortex," *Cereb. Cortex* **20**, 1293–1304 (2010).
- A. Pooresmaeili, J. L. Herrero, M. W. Self, P. R. Roelfsema, and A. Thiele, "Suppressive lateral interactions at parafoveal representations in primary visual cortex," *J. Neurosci.* **30**, 12745–12758 (2010).
- U. Polat and D. Sagi, "The relationship between the subjective and objective aspects of visual filling-in," *Vis. Res.* **47**, 2473–2481 (2007).
- C. D. Gilbert and T. N. Wiesel, "Morphology and intracortical projections of functionally characterised neurones in the cat visual cortex," *Nature* **280**, 120–125 (1979).
- K. S. Rockland and J. S. Lund, "Intrinsic laminar lattice connections in primate visual cortex," *J. Comp. Neurol.* **216**, 303–318 (1983).
- U. Polat, A. Sterkin, and O. Yehezkel, "Spatio-temporal low-level neural networks account for visual masking," *Adv. Cognit. Psychol.* **3**, 153–165 (2007).
- A. Sterkin, O. Yehezkel, Y. S. Bonneh, A. Norcia, and U. Polat, "Backward masking suppresses collinear facilitation in the visual cortex," *Vis. Res.* **49**, 1784–1794 (2009).
- J. A. Hirsch and C. D. Gilbert, "Synaptic physiology of horizontal connections in the cat's visual cortex," *J. Neurosci.* **11**, 1800–1809 (1991).
- L. J. Toth, S. C. Rao, D. S. Kim, D. Somers, and M. Sur, "Subthreshold facilitation and suppression in primary visual cortex revealed by intrinsic signal imaging," *Proc. Natl. Acad. Sci. USA* **93**, 9869–9874 (1996).
- L. M. Martinez, Q. Wang, R. C. Reid, C. Pillai, J. M. Alonso, F. T. Sommer, and J. A. Hirsch, "Receptive field structure varies with layer in the primary visual cortex," *Nat. Neurosci.* **8**, 372–379 (2005).
- J. G. Daugman, "Uncertainty relation for resolution in space, spatial frequency, and orientation optimized by two-dimensional visual cortical filters," *J. Opt. Soc. Am. A* **2**, 1160–1169 (1985).
- J. P. Jones and L. A. Palmer, "An evaluation of the two-dimensional gabor filter model of simple receptive fields in cat striate cortex," *J. Neurophysiol.* **58**, 1233–1258 (1987).
- H. Spitzer and S. Hochstein, "Simple-and complex-cell response dependences on stimulation parameters," *J. Neurophysiol.* **53**, 1244–1265 (1985).
- K. Naka and W. Rushton, "S-potentials from colour units in the retina of fish (cyprinidae)," *J. Physiol.* **185**, 536–555 (1966).
- J. Ross and H. D. Speed, "Contrast adaptation and contrast masking in human vision," *Proc. R. Soc. London Ser. A* **246**, 61–70 (1991).
- G. M. Boynton, J. B. Demb, G. H. Glover, and D. J. Heeger, "Neuronal basis of contrast discrimination," *Vis. Res.* **39**, 257–269 (1999).
- W. H. Bosking, Y. Zhang, B. Schofield, and D. Fitzpatrick, "Orientation selectivity and the arrangement of horizontal connections in tree shrew striate cortex," *J. Neurosci.* **17**, 2112–2127 (1997).
- D. J. Field, A. Hayes, and R. F. Hess, "Contour integration by the human visual system: evidence for a local association field," *Vis. Res.* **33**, 173–193 (1993).
- C. D. Gilbert and T. N. Wiesel, "Columnar specificity of intrinsic horizontal and corticocortical connections in cat visual cortex," *J. Neurosci.* **9**, 2432–2442 (1989).
- R. Malach, Y. Amir, M. Harel, and A. Grinvald, "Relationship between intrinsic connections and functional architecture revealed by optical imaging and in vivo targeted biocytin injections in primate striate cortex," *Proc. Natl. Acad. Sci. USA* **90**, 10469–10473 (1993).
- D. D. Stettler, A. Das, J. Bennett, and C. D. Gilbert, "Lateral connectivity and contextual interactions in macaque primary visual cortex," *Neuron* **36**, 739–750 (2002).
- H. B. Barlow, T. P. Kaushal, M. Hawken, and A. J. Parker, "Human contrast discrimination and the threshold of cortical neurons," *J. Opt. Soc. Am. A* **4**, 2366–2371 (1987).
- D. J. Tolhurst and A. F. Dean, "Spatial summation by simple cells in the striate cortex of the cat," *Exp. Brain Res.* **66**, 607–620 (1987).
- G. E. Legge, D. Kersten, and A. E. Burgess, "Contrast discrimination in noise," *J. Opt. Soc. Am. A* **4**, 391–404 (1987).
- J. Yang and W. Makous, "Modeling pedestal experiments with amplitude instead of contrast," *Vis. Res.* **35**, 1979–1989 (1995).
- L. L. Kontsevich and C. W. Tyler, "Bayesian adaptive estimation of psychometric slope and threshold," *Vis. Res.* **39**, 2729–2737 (1999).

50. W. A. Simpson, H. K. Falkenberg, and V. Manahilov, "A hard threshold in detection, summation, and direction discrimination?" *J. Vis.* **3**(9), 538 (2003).
51. M. Chirimuuta and D. Tolhurst, "Does a Bayesian model of V1 contrast coding offer a neurophysiological account of human contrast discrimination?" *Vis. Res.* **45**, 2943–2959 (2005).
52. G. E. Legge and J. M. Foley, "Contrast masking in human vision," *J. Opt. Soc. Am.* **70**, 1458–1471 (1980).
53. J. Gottesman, G. S. Rubin, and G. E. Legge, "A power law for perceived contrast in human vision," *Vis. Res.* **21**, 791–799 (1981).
54. G. E. Legge, "A power law for contrast discrimination," *Vis. Res.* **21**, 457–467 (1981).
55. B. M. Dow, A. Z. Snyder, R. G. Vautin, and R. Bauer, "Magnification factor and receptive field size in foveal striate cortex of the monkey," *Exp. Brain Res.* **44**, 213–228 (1981).
56. M. Y. Kwon, G. E. Legge, F. Fang, A. M. Y. Cheong, and S. He, "Adaptive changes in visual cortex following prolonged contrast reduction," *J. Vis.* **9**(2):20, 1–16 (2009).
57. J. F. Schumacher, S. K. Thompson, and C. A. Olman, "Contrast response functions for single gabor patches: ROI-based analysis over-represents low-contrast patches for GE BOLD," *Front. Syst. Neurosci.* **5**(19), 1–10 (2011).
58. L. Busse, A. R. Wade, and M. Carandini, "Representation of concurrent stimuli by population activity in visual cortex," *Neuron* **64**, 931–942 (2009).
59. Y. Yang, Z. Liang, G. Li, Y. Wang, Y. Zhou, and A. G. Leventhal, "Aging affects contrast response functions and adaptation of middle temporal visual area neurons in rhesus monkeys," *Neuroscience* **156**, 748–757 (2008).
60. D. C. Hood, Q. Ghadiali, J. C. Zhang, N. V. Graham, S. S. Wolfson, and X. Zhang, "Contrast-response functions for multifocal visual evoked potentials: a test of a model relating V1 activity to multifocal visual evoked potentials activity," *J. Vis.* **6**(5):4, 580–593 (2006).
61. J. Zheng, B. Zhang, H. Bi, I. Maruko, I. Watanabe, C. Nakatsuka, and Y. M. Chino, "Development of temporal response properties and contrast sensitivity of V1 and V2 neurons in macaque monkeys," *J. Neurophysiol.* **97**, 3905–3916 (2007).
62. J. L. Gardner, P. Sun, R. A. Waggoner, K. Ueno, K. Tanaka, and K. Cheng, "Contrast adaptation and representation in human early visual cortex," *Neuron* **47**, 607–620 (2005).
63. X. Li, Z. L. Lu, B. S. Tjan, B. A. Dosher, and W. Chu, "Blood oxygenation level-dependent contrast response functions identify mechanisms of covert attention in early visual areas," *Proc. Natl. Acad. Sci. USA* **105**, 6202–6207 (2008).
64. D. G. Albrecht and D. B. Hamilton, "Striate cortex of monkey and cat: contrast response function," *J. Neurophysiol.* **48**, 217–237 (1982).
65. A. Ishai and D. Sagi, "Visual imagery: effects of short-and long-term memory," *Cogn. Neurosci.* **9**, 734–742 (1997).
66. D. M. Green and J. A. Swets, *Signal Detection Theory and Psychophysics* (Wiley, 1966), Vol. 1.
67. J. M. Foley and G. E. Legge, "Contrast detection and near-threshold discrimination in human vision," *Vis. Res.* **21**, 1041–1053 (1981).
68. T. Ellenbogen, U. Polat, and H. Spitzer, "Chromatic collinear facilitation, further evidence for chromatic form perception," *Spat. Vis.* **19**, 547–568 (2006).
69. Y. Petrov, P. Vergheze, and S. P. McKee, "Collinear facilitation is largely uncertainty reduction," *J. Vis.* **6**(2), 170–172 (2006).
70. D. J. Heeger, "Normalization of cell responses in cat striate cortex," *Vis. Neurosci.* **9**, 181–197 (1992).
71. J. Xing and D. J. Heeger, "Measurement and modeling of center-surround suppression and enhancement," *Vis. Res.* **41**, 571–583 (2001).
72. Y. Barkan, H. Spitzer, and S. Einav, "Brightness contrast-contrast induction model predicts assimilation and inverted assimilation effects," *J. Vis.* **8**(7):27, 1–26 (2008).
73. E. Freeman, D. Sagi, and J. Driver, "Lateral interactions between targets and flankers in low-level vision depend on attention to the flankers," *Nat. Neurosci.* **4**, 1032–1036 (2001).
74. M. W. Cannon and S. C. Fullenkamp, "Spatial interactions in apparent contrast: inhibitory effects among grating patterns of different spatial frequencies, spatial positions and orientations," *Vis. Res.* **31**, 1–26 (1991).
75. Y. Petrov and S. P. McKee, "The effect of spatial configuration on surround suppression of contrast sensitivity," *J. Vision* **6**(3):224–238 (2006).
76. M. Kilpeläinen, K. Donner, and P. Laurinen, "Time course of suppression by surround gratings: highly contrast-dependent, but consistently fast," *Vis. Res.* **47**, 3298–3306 (2007).
77. L. Schwabe, K. Obermayer, A. Angelucci, and P. C. Bressloff, "The role of feedback in shaping the extra-classical receptive field of cortical neurons: a recurrent network model," *J. Neurosci.* **26**, 9117–9129 (2006).
78. J. M. Ichida, L. Schwabe, P. C. Bressloff, and A. Angelucci, "Response facilitation from the 'suppressive' receptive field surround of macaque V1 neurons," *J. Neurophysiol.* **98**, 2168–2181 (2007).
79. W. Bair, J. R. Cavanaugh, and J. A. Movshon, "Time course and time-distance relationships for surround suppression in macaque V1 neurons," *J. Neurosci.* **23**, 7690–7701 (2003).